Implementation of Inverse Kinematics for Crop-Harvesting Robotic Arm in Vertical Farming

Sandy C. Lauguico
De La Salle University
Manila, Philippines
sandy_lauguico@dlsu.edu.ph

Ronnie S. Concepcion II
De La Salle University
Manila, Philippines
ronnie_concepcionii@dlsu.edu.ph

Dailyne D. Macasaet
De La Salle University
Manila, Philippines
dailyne_macasaet@dlsu.edu.ph

Jonnel D. Alejandrino
De La Salle University
Manila, Philippines
Jonnel_alejandrino@dlsu.edu.ph

Argel A. Bandala
De La Salle University
Manila, Philippines
argel_bandala@dlsu.edu.ph

Elmer P. Dadios
De La Salle University
Manila, Philippines
elmer_dadios@dlsu.edu.ph

***Abstract*— The world population is expected to increase to 9.8 billion in 2050 according to United Nations. With this, scarcity of food and space will further be a major concern. This study proposes a framework which used initializing, processing, and directing applied to an inverse kinematics based robotic arm. An automatized approach in addressing the foreseeable problem on providing nutritional plant-based food considering that cities are becoming highly-urbanized was developed. Wall gardening used for vertical farming or urban farming is a technique by which there are sets of rows and columns of pockets installed over a wall. These pockets are filled with soil or other planting bases (i.e. water for hydroponics) for the seedlings to grow. A robotic arm is manually set to point on a specific pocket where a crop has grown. Using inverse kinematics, the set points determine the joint angles. This then targets the pockets and the end-effector of the robot arm performs a grip to the roots of the crops. The robotic arm then moves to its initial point, technically pulling up the crop. After positioning to the initial point, the arm directs to the side of the wall, where a container is located. The end-effector opens to drop the crop carefully into the container. The research study is simulated using MATLAB and Universal Robots. The results show that it can only yield 85.42% of the crops.**

Keywords— inverse kinematics, robotic arm, wall gardening, vertical farming

I. INTRODUCTION

Vertical farming is becoming more relevant in urban areas and encouraged to be done in homes as it has been a concern that transporting fruits and vegetables for over long distances (from the provinces to the cities) lose a significant amount of nutrients along the way [1]. Crop transportation becomes more expensive over time as well especially when there are delays in delivery [2]. Another significance of vertical farming is that production of specific crops will not be affected much by seasonal change and environmental factors as they are mostly indoors [3]. In the near future, this method of farming will be more important as the number of population increases – which results to scarcity in space and production. Thus, the study of this method of urban farming will soon be essential to mankind. Furthermore, it will possibly lead to researches that will support food production outside of earth. The further study of this applied to urban farming becomes significant as space studies [4][5] on alternative human habitat are booming, implying that farming can be done anywhere.

However, vertical farming cannot be optimized without automation [6]. Some of the crops cannot be easily harvested because they are out of reach as wall gardens are usually high. It would also take more time to harvest if the crops are yielded without path planning. Automating such tasks would be a promising solution for crop yielding.

The main objective of the study is to develop a framework for optimizing a robot arm for harvesting crops in vertical farming, specifically on a wall garden setup. The research is specifically aiming to utilize inverse kinematics in order to increase the precision of the actuator's position derived from the right combination of every joint's angle. Another specific purpose is to determine the best path for which the inverse kinematics is configured to direct the actuator's route.

The discussions in this paper are divided into seven more sections. Section II and III dicsuss about related studies and inverse kinematics respectively. Section IV is regarding the conceptual framework proposed. Section V presents the implementation of inverse kinematics to the robotic arm simulation using both MATLAB and Universal Robot. Section VI deals with testing while Section VII is about the results of the implementation. Section VIII gives off the conclusion and future recommendations.

II. RELATED STUDIES

One of the most invested and researched methods for automation, especially in agriculture, is the use of machinery powered by robotic applications. This provides precision on operating, controlling, and guiding machines to efficienctly perform agricultural tasks [7]. Such significance of robotics to agriculture has been very evident that a study on making actuators adaptable and flexible was done [8] in oder to avoid

978-1-7281-3458-1/19/$31.00 ©2019 IEEE

damaging crops because of the high pressure bought by rock-solid robot parts.

With these, the use of robotics in the field of agriculture, specifically in vertical farming is becoming more relevant and considered practical. Some of the robots were designed for harvesting specific crops. A robot was designed for harvesting spherical fruits through multi-sensing in its end-effector. It has a two-finger gripper, vacuum suction pad device, and a laser-cutting device to make sure that the fruit will not be forced for gripping and avoid damage [9]. A binocular vision-based tomato-harvesting robot was also designed. A Raspberry Pi controls the mobile vehicle and the mechanical arm through the data gathered from a binocular camera [10]. Another robot for yielding strawberries, being grown in ridge culture, was devised with four joints to moved in parallel with the ridge [11]. A design of wolfberry picking robot was implemented with sensors, camera, and picking manipulators [12].

III. INVERSE KINEMATICS

Kinematics or forward kinematics, applied in manipulating robotic arms, is a mathematical approach for relating the position of the end-effector with the angles of the joints [13]. Angles of the joints are initially set and used as input data to solve for the posture of the end-effector. The process of the solving is defined as forward kinematics analysis. This can be presented by equation 1.

$$X_{EE} = \mathrm{f}(\theta) \tag{1}$$

Where X_{EE} is the end effector position and (θ) is the state vector in the joint (angular) space.

The mathematics behind inverse kinematics is simply applying forward kinematics the other way around. Instead of providing the position of the end-effector from given joints' angles, the end-effector's positions are initially set to derive what should be the angle of the joints depending on the degree of freedom of the robot arm [14]. The mathematical equation that represents inverse kinematics is shown in equation 2.

$$(\theta) = f^{-1}(X_{EE}) \tag{2}$$

Where (θ) is the state vector in the joint (angular) space and X_{EE} is the end effector position.

It can be observed that the dependent and independent variables from forward kinematics are just interchanged to get the equation that models inverse kinematics. This makes the use of inverse kinematics essential to easily set using manual configurations the target points for the vertical farm pockets. This further provides precise end-effector posture and position for making sure that the gripper can specifically capture the crops from the pockets.

Figure 1 shows the 3R elbow-type arm of a Univeral Robot that was used for the implementation of the inverse kinematics studied and derived on this paper. Shown in equation 3 represents how the joints move in accordance to the positions serving as inputs.

$$p_x{}^2 + p_y{}^2 + (P_z - d_1)^2 = C_1{}^2(L_2C_2 + L_3C_{23})^2 + s_1{}^2(L_2C_2 + L_3C_{23})^2 + (L_2C_2 + L_3C_{23})^2 \tag{3}$$

Where p is the position with respect to the x and y axis, d is the length of the base part of the arm, l is the length of the arms connected to the base and actuator, and c and s are values derived from equations 4 and 5 respectively [15].

$$c_3 = (p_x{}^2 + p_y{}^2 + (P_z - d_1)^2 - L_2{}^2 - L_3{}^2) / 2\,L_2L_3 \tag{4}$$

$$\pm s_3 = \pm \sqrt{1 - C_3{}^2} \tag{5}$$

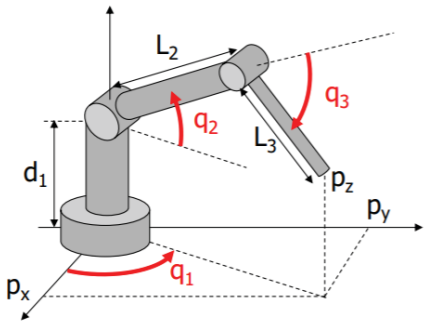

Fig. 1. Universal Robot Diagram

A study on a five-joint robot utilized an inverse kinematics solution to set the end-effector's position and orientation as input data for training a neural network [16]. This results to effectively formulating and simulating the network because of the precise input data from the inverse kinematics solution. Aside from precision, using an inverse kinematics function, provides a faster solution for setting the angles of the joints, which lead to the targeting and pulling of crops movements smooth. Inverse kinematics solution applied in a hybrid manipulator is used for connecting serially a binary manipulator with a manipulator that is parallel [17], providing an optimized path profile for the actuator movements to different waypoints.

There are specific studies on robots that use inverse kinematics for performing agricultural tasks. Such studies are watermelon picking robot that is controlled by Genetic Algorithm (GA)-based solution inverse kinematics [18], an inverse kinematics driven servoing agriculture robot through visual controls [19], a robot arm that relies on depth sensors and inverse kinematics for motion to do agricultural applications [20], and a coconut robot harvester fabricated with four degrees of freedom using inverse kinematics calculation [21].

These studies prove the significance of using inverse kinematics for automating crop-harvesting using robot arm in terms of optimization. These important aspects of precision and fast calculation ensure the arm to hit the target pockets, effectively pull the crops from the wall, and place them in a specifically-located container while considering the best path to take.

IV. CONCEPTUAL FRAMEWORK

A summaru of the system flow is shown in Figure 2 for the robot arm to take motion as proposed. The system is divided into three main parts: initializing, processing, and directing. The first part starts with the robot arm initialized at a neutral location from the wall garden. Once initialized, waypoints are manually set to serve as the data for determining the desired target points. The coordinates of the waypoints set are used as input paramterers.

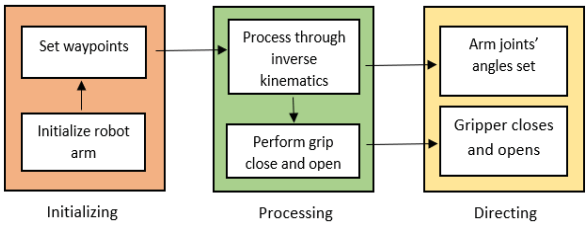

Fig. 2. Conceptual Framework

These input parameters are then processed through inverse kinematics to solve for the angles of the joints to attain the designated position and posture of the end-effector. As the end-effector is placed to its target, the gripper is set to perform close.

The output of the inverse kinematics are sets of joint angles which set the end-effector to a specific row and column along with a specific posture. Once there, the gripper closes to grab a crop. The next set of angles directs the end-effector to the initialized or neutral location. Then the next set of angles from the inverse kinematics directs the end-effector to a location away from the wall garden where a container is located. As it gets there, the gripper performs an open to drop off the crop. The process repeats as the waypoint ends at the initial point.

V. IMPLEMENTATION OF INVERSE KINEMATICS

Implementing inverse kinematics to the robot arm was performed through both software and hardware. The software part was implemented using MATLAB R2018b, while the hardware implementation was done through Universal Robot (UR). The software allowed to initially simulate the derived inverse kinematics from a set of waypoints to ensure the workability of the mathematical equations. The application on the hardware on the other hand, was able to consider physical factors that may affect the optimization from the equations used.

A. Implementations of Inverse Kinematics Using MATLAB

For initially setting up of the implementation, a rigid body tree variable was used to display a robot arm. A dimension-defined space was also set up as to where the end-effector moved along specific coordinates.

Input parameters were detailed in a waypoint variable. The coordinates were three-dimensional for setting up a 4x3 matrix for twelve target pcokets. The central or neutral point was also set once every after target of a specific row-column, making a total of 24 points for where the end-effector aims to move.

The specific waypoints for each target pocket were:

$$\begin{bmatrix} 0.3\ 0.1\ 0.25 & 0.3\ -0.1\ 0.25 & 0.3\ -0.3\ 0.25 \\ 0.3\ 0.1\ 0.2 & 0.3\ -0.1\ 0.2 & 0.3\ -0.3\ 0.2 \\ 0.3\ 0.1\ 0.15 & 0.3\ -0.1\ 0.15 & 0.3\ -0.3\ 0.15 \\ 0.3\ 0.1\ 0.1 & 0.3\ -0.1\ 0.1 & 0.3\ -0.3\ 0.1 \end{bmatrix}$$

The coordinate for the neutral point is [0.1 0 0.175], which was placed every after coordinate for displaying a pull for the crop. These coordinates were processed through a built-in inverse kinematics function in MATLAB using the equations preented so that the trajectory of the arm was reflected as it moved from point to point. The function underwent a series of codes to effectively integrate it to the rigid body used for waypoint simulations.

From Figure 3, the twelve blue points represent the target pockets of where the crops are individually planted vertically. It can be seen that the arm rests on a point away from the blue points. That is the neutral or initial point where arm goes back after hitting one pocket, effectively pulling the crop. The red lines show the trajectory of the end-effector's motions.

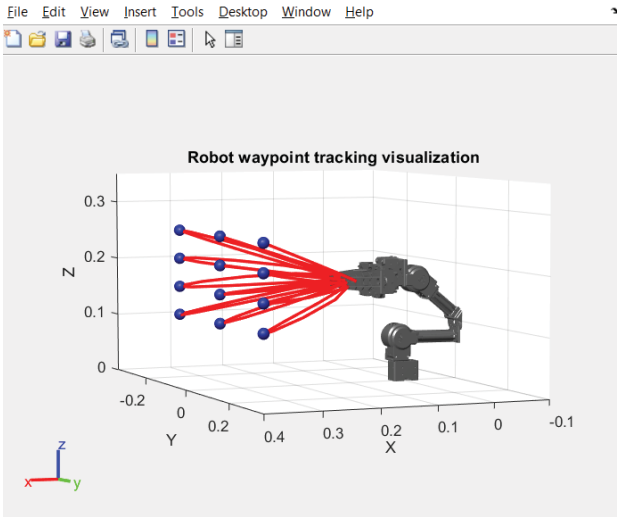

Fig. 3. MATLAB Simulation

B. Implementations of Inverse Kinematics Using Universal Robot

The hardware implementation was set by initializing the end-effector to its neutral point similar to the software simulation. The waypoints were set by maually by moving the UR's arm to points that serve as target pockets. These waypoints are paralleled and proportioned with the waypoints set in MATLAB.

The green pencils from Figure 4 were the blue points equivalent for the software model.

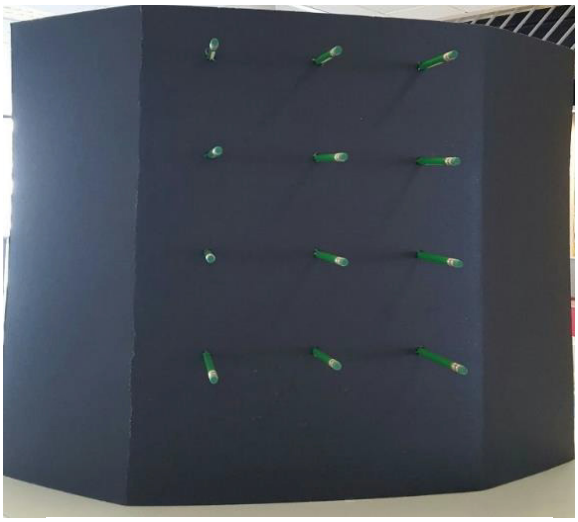

Fig. 4. Wall Garden Props Illustration

As three-dimensional, the pencils served as representation for crops planted to a specific pocket. They only represent the crop locations and not necessarily representing the rigidity of crops. The pencils were placed in four rows and three columns in dimensions proportion to the software simulation coordinates.

Represented in Figure 5 was the set up of the UR end-effector facing up the wall garden props. Shown there was the arm positioned at the initial or neutral point. The grip was open also as shown because it was not yet gripping on a pencil.

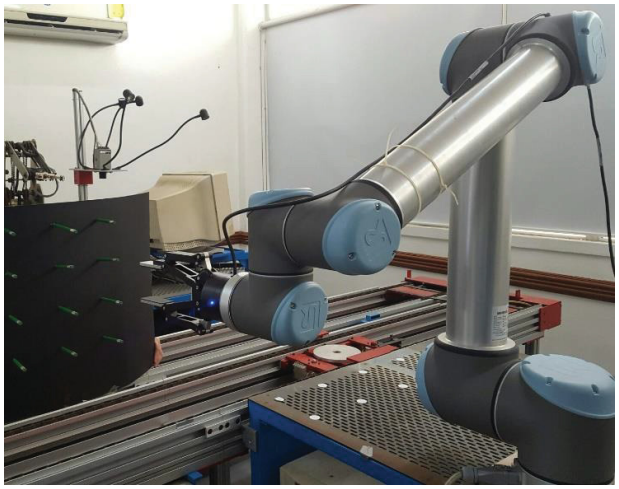

Fig. 5. UR and Wall Garden Props Setup

The first movement of the arm aimed to row 1 column 1 (R1C1). The gripper then performed a close to inilialize the grab gesture for the pencil. It then proceeded to going back to its neutral point, while holding the pencil, effectively pulling the pencil from the pocket. The next movement was to the side of the props where a container was located. The gripper performed an open to drop the pencil and immediately went back to neutral point. The cycle went on by aiming R1C2, completing the first row first before proceeding to the second row. The movement was made possible by the UR by having inverse kinematics process the waypoints to set the arms' joints angles in order to provide the specific position and posture of the end-effector.

A sample of a reading of the set of angles for a specific joint is shown in Figure 6.

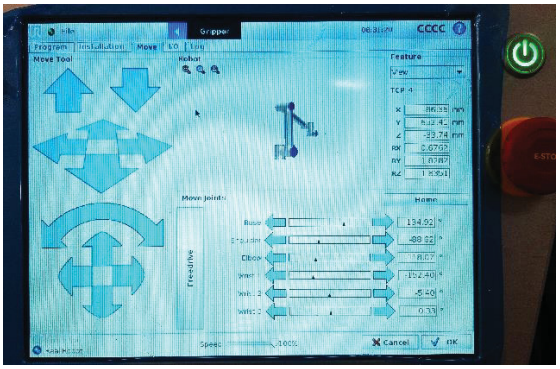

Fig. 6. Sample Joint Angle Reading

The reading is shown via the UR monitor which is also used for setting up the waypoints and the sequence of movements, technically the program input of the robotic arm. The set of angles for each joint collectively and effectively direct the end-effector to the pockets, the neutral point, and the container.

Table 1 shows the angles of each six joints namely: base, shoulder, elbow, wrist 1, wrist 2, and wrist 3.

TABLE I. JOINT ANGLES

Joints	**Neutral**	**R1C1**	**R1C2**	**R1C3**
Base	134.92	99.23	96.30	91.24
Shoulder	-88.62	-119.62	-115.13	-111.48
Elbow	-118.07	-73.49	-77.04	-81.80
Wrist 1	-152.40	-160.70	-170.27	-168.88
Wrist 2	-5.40	-34.68	-32.18	-32.19
Wrist 3	0.33	-0.07	-0.05	0.00
Joints	**Container**	**R2C1**	**R2C2**	**R2C3**
Base	106.33	100.86	96.27	87.85
Shoulder	-157.70	-130.70	-117.85	-110.66
Elbow	-24.97	-60.30	-90.57	-96.80
Wrist 1	-189.74	-184.52	-136.39	-149.76
Wrist 2	-92.01	-22.27	-31.31	-48.36
Wrist 3	-112.06	22.32	-13.98	-14.00
Joints	**R3C1**	**R3C2**	**R3C3**	
Base	100.26	96.01	88.02	
Shoulder	-126.64	-120.92	-115.04	
Elbow	-87.16	-91.39	-98.55	
Wrist 1	-131.98	-144.51	-148.52	
Wrist 2	-33.98	-32.76	-46.32	
Wrist 3	-13.99	-13.98	-13.96	
Joints	**R4C1**	**R4C2**	**R4C3**	
Base	99.43	93.81	85.98	
Shoulder	-132.68	-126.24	-120.85	
Elbow	-88.83	-99.64	-107.61	
Wrist 1	-122.25	-123.22	-123.22	
Wrist 2	-34.81	-43.74	-55.00	
Wrist 3	-13.96	-13.96	-13.96	

These angles represent the inverse kinematics output from the initialized waypoints. Having these angles, the end-effector aims automatically for the manually designated desired target pockets and locations, which are represented by Neutral, Container, R1C1, R1C2, R1C3, and so on. Therefore, completing 14 aiming points.

VI. TESTING

Through the hardware simulation, there are four testing classifications done, namely Testing Classification A up to D. Each testing classification is uniquely defined by the pocket sequence of waypoints which the arm follows without altering the originally initialized waypoints. This is also defined as the planned path for the arm's movements. The most number of pulled pencils (crops) among the path planned classification will be considered as the most effective way to set the waypoints in order to process them as input parameters for the inverse kinematics to efficiently produce the desired angles for the joints.

Software testing using the four testing classifications was not done because the set of joint angles are perfectly following the set waypoints because it does not reflect the external factors of the system that would possibly lead to inefficiently following the path. Such factors considered are the different level of thightness the pencils are in pockets

(technically the thightness of the crops' roots to the pockets), the robot arm force, and the steadiness of the wall garden.

Table II shows one of the testing classifications used, specifically A. The sequence shown is the waypoints of the pockets which are arranged in such a way that the end-effector starts pulling off all the pockets in the first row before proceeding with second row, the third, and finally the forth; by which all the row movement goes from left to right.

TABLE II. TESTING CLASSIFICATION A

Gripper Open	center
center	r3c1
r1c1	Gripper Close
Gripper Close	center
center	container
container	Gripper Open
Gripper Open	center
center	r3c2
r1c2	Gripper Close
Gripper Close	center
center	container
container	Gripper Open
Gripper Open	center
center	r3c3
r1c3	Gripper Close
Gripper Close	center
center	container
container	Gripper Open
Gripper Open	center
center	r4c1
r2c1	Gripper Close
Gripper Close	center
center	container
container	Gripper Open
Gripper Open	center
center	r4c2
r2c2	Gripper Close
Gripper Close	center
center	container
container	Gripper Open
Gripper Open	center
center	r4c3
r2c3	Gripper Close
Gripper Close	center
center	container
container	Gripper Open
Gripper Open	center

Note: The sequence of the script is read vertically from top to bottom, then proceeding to the right column of the table. The r and c, center, and container are the waypoints where the actuators are directed.

Testing Classification B is similar to A, but instead of row movement, it does column movement. It is starting off fully pulling all the pencils from the first column first before proceeding to the second and third column. All column movement goes from the top going downward.

The sequence for Testing Classification C is that the waypoints start moving from left to right on the first row. Upon reaching the third column of the third row, it moves downward to the second row and proceeding to move from right to left. It then cyclically continues to its first movement once reaching the third row.

Like C, Testing Classification D moves alternatingly. It starts moving downward on the first column starting from R1C1. Reaching R3C1, it proceeds to R3C2 then starts moving upward. On the third column, it moves downward again, finally completing all the 12 pockets.

The center and container points sequence are fixed. Everytime it aims a pocket, the next movement is the center and container respectively. It then proceeds to the next pocket depending on what tecting classification is set.

VII. RESULTS AND DISCUSSION

The results are summarized by having all four testing classifications used for sequencing the pulling of the pencil for each pocket. The data shown are the modes of ten testings done for each classification. The mode signifies that at least seven out of ten testings done are producing consistent results.

TABLE III. SUCCESS OR FAIL OF THE PENCIL PULLING

Classification	**R1C1**	**R1C2**	**R1C3**
A	1	1	1
B	1	1	1
C	1	1	1
D	1	1	1
Classification	**R2C1**	**R2C2**	**R2C3**
A	1	1	1
B	1	1	0
C	0	1	1
D	1	1	1
Classification	**R3C1**	**R3C2**	**R3C3**
A	1	0	1
B	1	1	1
C	1	1	1
D	0	1	1
Classification	**R4C1**	**R4C2**	**R4C3**
A	0	1	1
B	1	1	1
C	1	1	1
D	1	0	0

Note: 1 represents that the end-effector successfully pulled the pencil from the pocket. 0 represent that the end-effector failed on pulling the pencil from the pocket.

As seen, the number of times the end-effector successfully pulled the pencil from the pcoket (which represents the harvesting of the crop) ranges from 9 to 11 for each classification.

TABLE IV. SUMMARY OF RESULTS

Classification	**No. of Successful Pulls**
A	10
B	11
C	11
D	9

Out of 12 pockets, Testing Classification A has a success rate of 83.335, B and C both have 91.67% success rate, and D has 75% success rate of pulling up the the pencils from the pockets.

These averages to 85.42% rate of successfully gripping and pulling up the pencils from the pockets, which demonstrates effectively harvesting the crop from where its planted in a wall garden. From the summary, it shows the Testing Classification B and C are the most effective sequence. However, B is a column movement while C is a

row movement. Emphasizing this, gives the idea that sequencing of waypoints does not contribute for the success rate of the end-effector to take hold of a pencil technically based on equations, but it still compensates to the effects of external factors.

The target points where the end-effector is set are always successfully targeted in a perfect environment. The failing part of tests are results of external factors. The most contributing factor for failure is the wall garden being not stable because it gets moved due to the strong force of the robot arm.The neutral and container points are always aimed by the end-effector without problem.

VIII. CONCLUSION AND RECOMMENDATION

Based on the results of the evaluations done with the framework proposed, the set of waypoints used as input parameters processed through inverse kinematics, precisely set the needed angle of the robot's arm joints. The 14.58% failing rate of the pulling up of the pencil by the gripper was a result of external factors on the crop tightness to the pocket, the robotic arm's force, and the wall garden's stability. Inverse kinematics-wise, the end-effector is properly positioned and postured on the set targets all the time. For the path planning, classification B and C were able to yield 11 out of 12 pencils, implying 91.67% effectivity on the actuators' movements to meet the objectives. This route can be obtained in an actual vertical farm set up to optimize the yielding of crops by which the end-effector's sequence of movements for harvesting.

This sums up to an implementation of initializing, processing, and directing of an inverse kinematics based optimized robotic arm aiming a specific pocket on a wall garden at the best path profile option. The automation of harvesting of crops is effectively done both in software and hardware implementation.

However, the output is not the same for both because of the external factors. Despite the proper positioning and posturing of the end-effector, it is recommended that the contributing factors for failure in hardware are addressed. The major factor among the three is the steadiness of the wall garden because of the robot's force. Another factor to be considered is the thightness of the roots of the crops in the soil or other planting bases.

ACKNOWLEDGEMENT

The researchers would like to thank the Engineering Research and Development Technology (ERDT) of the Department of Science and Technology (DOST) of the Philippines and the De La Salle University (DLSU) Intelligent Systems Laboratory (ISL) for the support they provided.

REFERENCES

[1] F. C. L. Belista, M. P. C. Go, L. L. Lucenara, C. J. G. Policarpio, X. J. M. Tan, and R. G. Baldovino, "A smart aeroponic tailored for IoT vertical agriculture using network connected modular environmental chambers," 2018 IEEE 10th Int. Conf. Humanoid, Nanotechnology, Inf. Technol. Commun. Control. Environ. Manag. HNICEM 2018, pp. 4–7, 2019.

[2] A. Abderrahman, E. H. A. Ahmed, and B. Jaouad, "Intermodal transport of vegetables from Morocco to Europe," Proc. 3rd IEEE Int. Conf. Logist. Oper. Manag. GOL 2016, pp. 1–5, 2016.

[3] S. S. S. Yusof, N. M. Thamrin, M. K. Nordin, A. S. M. Yusoff, and N. J. Sidik, "Effect of artificial lighting on typhonium flagelliforme for indoor vertical farming," Proc. - 2016 IEEE Int. Conf. Autom. Control Intell. Syst. I2CACIS 2016, no. October, pp. 7–10, 2017.

[3] B. V Aishwarya and G. Archana, "Agriculture Robotic Vehicle Based Pesticide Sprayer With Efficiency Optimization," 2015 IEEE Technol. Innov. ICT Agric. Rural Dev., no. Tiar, pp. 59–65, 2015.

[4] M. Simon et al., "NASA's advanced exploration systems Mars transit habitat refinement point of departure design," IEEE Aerosp. Conf. Proc., pp. 1–34, 2017.

[5] M. L. Gernhardt et al., "Mars ascent vehicle sizing, habitability, and commonality in NASA's evolvable mars campaign," IEEE Aerosp. Conf. Proc., pp. 1–19, 2017.

[6] A. V. David, H. T. Mohan, and R. R. Bhavani, "Design and modelling of a cable driven cart-rail robot for farm automation," 2017 Int. Conf. Intell. Comput. Instrum. Control Technol. ICICICT 2017, vol. 2018–Janua, pp. 1248–1253, 2018.

[7] F. A. Auat Cheein and R. Carelli, "Agricultural robotics: Unmanned robotic service units in agricultural tasks," IEEE Ind. Electron. Mag., vol. 7, no. 3, pp. 48–58, 2013.

[8] G. Bao, P. Yao, S. Cai, S. Ying, and Q. Yang, "Flexible pneumatic end-effector for agricultural robot: Design & experiment," 2015 IEEE Int. Conf. Robot. Biomimetics, IEEE-ROBIO 2015, pp. 2175–2180, 2015.

[9] J. Liu, P. Li, and Z. Li, "A multi-sensory end-effector for spherical fruit harvesting robot," Proc. IEEE Int. Conf. Autom. Logist. ICAL 2007, pp. 258–262, 2007.

[10] T. Zhou, D. Zhang, M. Zhou, H. Xi, and X. Chen, "System Design of Tomatoes Harvesting Robot Based on Binocular Vision," Proc. 2018 Chinese Autom. Congr. CAC 2018, pp. 1114–1118, 2019.

[11] K. Zhang, T. Zhang, and D. Zhang, "Synthesis design of a robot manipulator for strawberry harvesting in ridge-culture," Proc. 2016 Asia-Pacific Conf. Intell. Robot Syst. ACIRS 2016, pp. 114–117, 2016.

[12] X. Zhang et al., "Study on the design and control system for wolfberry harvesting robot," Proc. 28th Chinese Control Decis. Conf. CCDC 2016, pp. 5984–5985, 2016.

[13] Z. Jin and Y. Chao, "Kinematics and differential kinematics of an articulated heavy load carrying robot," Proc. 2016 IEEE 11th Conf. Ind. Electron. Appl. ICIEA 2016, vol. 15, pp. 107–112, 2016.

[14] P. Srisuk, A. Sento, and Y. Kitjaidure, "Inverse kinematics solution using neural networks from forward kinematics equations," 2017 9th Int. Conf. Knowl. Smart Technol. Crunching Inf. Everything, KST 2017, pp. 61–65, 2017.

[15] "Robotics 1: Inverse Kinematics" [Online]. Available: http://www.diag.uniroma1.it/~deluca/rob1_en/10_InverseKinematics.pdf [Accessed 26 June 2019]

[16] D. R. Raj, I. J. Raglend, and M. D. Anand, "Inverse kinematics solution of a five joint robot using feed forward and Radial Basis Function Neural Network," 4th IEEE Spons. Int. Conf. Comput. Power, Energy, Inf. Commun. ICCPEIC 2015, pp. 117–122, 2015.

[17] K. Maeda and E. Konaka, "Inverse kinematics solution algorithm for continuous/binary hybrid manipulator," IEEE Int. Conf. Autom. Sci. Eng., vol. 2015–October, pp. 483–488, 2015.

[18] Z. Zou, J. Han, and M. Zhou, "Research on the inverse kinematics solution of robot arm for watermelon picking," Proc. 2017 IEEE 2nd Inf. Technol. Networking, Electron. Autom. Control Conf. ITNEC 2017, vol. 2018-January, pp. 1399–1402, 2018.

[19] T. Dewi, P. Risma, Y. Oktarina, and S. Muslimin, "Visual Servoing Design and Control for Agriculture Robot; A Review," Proc. 2018 Int. Conf. Electr. Eng. Comput. Sci. ICECOS 2018, vol. 17, pp. 57–62, 2019.

[20] R. K. Megalingam, G. V. Vivek, S. Bandyopadhyay, and M. J. Rahi, "Robotic arm design, development and control for agriculture applications," 2017 4th Int. Conf. Adv. Comput. Commun. Syst. ICACCS 2017, 2017.

[21] S. Parvathi and S. T. Selvi, "Design and fabrication of a 4 Degree of Freedom (DOF) robot arm for coconut harvesting," Proc. 2017 Int. Conf. Intell. Comput. Control. I2C2 2017, vol. 2018-January, pp. 1–5, 2018.